Journal of King Saud University – Science 35 (2023) 102475

HOSTED BY

Contents lists available at ScienceDirect

Journal of King Saud University – Science

journal homepage: www.sciencedirect.com

Original article

Catalytic multicomponent synthesis, biological evaluation, molecular docking and in silico ADMET studies of some novel 3-alkyl indoles

Rajalakshmi Ramarajan [a,*], Arulraj Ramalingam [b,*], Chinnaraja Duraisamy [c], Sivakumar Sambandam [d,e], Noureddine ISSAOUI [f,*], Omar M. Al-Dossary [g,*], Leda G. Bousiakoug [h]

[a] Department of Chemistry, Annamalai University, Annamalainagar, Tamil Nadu 608 002, India
[b] Department of Electrical and Computer Engineering, National University of Singapore, 117 583, Singapore
[c] Department of Chemistry, PRIST University, Thanjavur, Vallam, Tamil Nadu 613 403, India
[d] Research and Development Centre, Bharathiar University, Coimbatore, Tamil Nadu 641 046, India
[e] BPJ College of Arts and Science, Kozhai, Srimushnam, Cuddalore 608703, Tamil Nadu, India
[f] University of Monastir, Faculty of Sciences, Laboratory of Quantum and Statistical Physics (LR18ES18), Monastir 5079, Tunisia
[g] Department of Physics and Astronomy, College of Science, King Saud University, PO Box 2455, Riyadh 11451, Saudi Arabia
[h] IMD Laboratories Co, R&D Section, Lefkippos Technology Park, NCSR Demokritos, PO Box 60037, 15130 Athens, Greece

ARTICLE INFO

Article history:
Received 12 October 2022
Revised 3 November 2022
Accepted 27 November 2022
Available online 5 December 2022

Keywords:
3-Alkylated indoles
Multicomponent reaction
Antimicrobial studies
Molecular docking
In silico ADMET

ABSTRACT

A series of novel 3-alkylated indoles were synthesized in good yields under mild reaction conditions using inexpensive, readily available, and environmentally benign glycolic acid catalyst. This new catalytic multicomponent reaction is attractive for diversity-oriented synthesis involving C–C bond formation. This strategy has a number of advantages, such as a simple work-up procedure, and short reaction time. Antimicrobial studies were carried out and the *para*-nitro-substituted compounds were found to be good inhibitors of *Aspergillus niger*. This activity explained by interacting with active site residues such as MET816, PHE786, and PHE820 of the target fungal protein, phosphodiesterase-5 (PDE5) (PDB:2H44). Furthermore, the SwissADME online application was used to analyses the physicochemical and pharmacokinetic features of the compounds (**6–10**).

1. Introduction

3-Alkylindoles have high biological activities (Oh et al., 2005) and are widely used in the synthesis of natural products, pharmaceuticals, functional materials, and agrochemicals (Glennon et al., 2000; Shaikh et al., 2008; Luk et al., 2011). Substituted indoles are capable of binding to many receptors with high affinity. The indole nucleus is an important structural unit that is present in a number of drugs currently on the market (Sundberg, 1996; Garbe et al., 2000). Most of these belong to the 3-substituted indole derivatives, which are an important intermediate for organic synthesis and are widely distributed in many natural products (John Faulkner, 1999). Consequently, the synthesis and selective functionalization of indoles have been the focus of lots of valuable research. The 3-substituted indoles are significant structural blocks for the synthesis of a variety of bioactive molecules, many of which are found in nature, which exhibit useful biological properties (Srivastava and Banik, 2003), such as antioxidant, antibacterial, insecticidal, and anticancer activity (Wenkert et al., 1986; Yoshiaki et al., 2002). Recently, there has been a great deal of research interest in the synthesis of these compounds due to their wide range of biological activities. Indole nucleus-containing drugs, such as sumatriptan, frovatriptan, zolmitriptan and rizatriptan, are used for the treatment of migraine headaches (Wynne and Stalick, 2002; Wang et al., 2010), whereas azolylbenzyl indole and bis-indole are used in the treatment of breast cancer and as an HIV-1 integrase inhibitor, respectively (Fig. 1) (Lézé et al., 2004).

By employing using powerful carbon–carbon bond forming reactions, synthesis of 3-substituted indole derivatives was achieved using the Mannich reaction (Campos et al., 2004), Friedel–Crafts alkylation (Zhao et al., 2006) of indoles and conjugate addition of indoles to unsaturated carbonyl compounds, and the

* Corresponding authors.
E-mail addresses: chemrajalaksmi@gmail.com (R. Ramarajan), rarulraj108@gmail.com (A. Ramalingam), issaoui_noureddine@yahoo.fr (N. ISSAOUI), omar@ksu.edu.sa (O.M. Al-Dossary).

Peer review under responsibility of King Saud University.

Production and hosting by Elsevier

https://doi.org/10.1016/j.jksus.2022.102475
1018-3647/

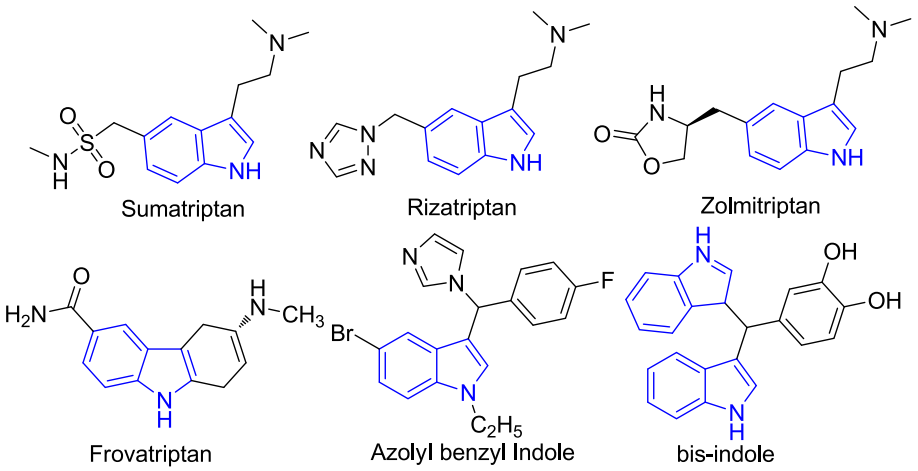

Fig. 1. Chemical structures of some biologically active 3-substituted indoles.

reaction of two equivalents of indoles with carbonyl groups in the presence of a protic acid (Reddy et al., 2003) or Lewis acid (Babu et al., 2000; Nagarajan and Perumal, 2002). Notably, 3-substituted indole derivatives containing nitrogen atoms have not been explored. Synthesis of these compounds containing nitrogen atoms is highly desirable because they may exhibit interesting pharmacological activities (Vardanyan and Hruby, 2006).

Multicomponent reactions (MCRs), where at least three reactants are added together in a single pot to yield various bioactive heterocyclic compounds, play important roles in synthetic organic chemistry (de Graaff et al., 2012; Dömling et al., 2012). There is increasing interest in MCRs with environmentally benign processes, and they have been achieved by consecutive reactions in water (Ollevier et al., 2006), ionic liquids (Sheldon, 2001), or under solvent-free conditions (Raston and Scott, 2000). Glycolic acid is an inexpensive, easy to handle, and environmentally friendly catalyst, but there have been no previous reports on glycolic acid catalyzed synthesis of indolylanilines. Therefore, we planned catalyzed synthesis of cyanoindolylanilines to develop useful methods for synthesis of drug-like molecules and pharmaceutical intermediates.

2. Materials and methods

All chemicals and solvents were bought from Sigma-Aldrich with a high degree of purity, and the chemicals used in the synthesis required no additional purification. We optimized three-component reactions of equimolar amounts of 5-cyanoindole, aryl-aldehyde, and aryl-amine in CH_3CN. To optimize the conditions, the reaction was carried out with various oxidants and glycolic acid in different solvent systems including EtOH, MeOH, toluene, tetrahydrofuran, *N,N*-dimethylformamide and acetonitrile.

2.1. Spectral characterization

All reported melting points were recorded in open glass capillaries on SUNTEX melting point apparatus and are given uncorrected. The IR spectra were recorded on an AVATAR-330, FT-IR spectrophotometer and only noteworthy absorption levels (reciprocal centimeters) are listed. ^{1}H NMR spectra were recorded at 400 and 500 MHz on a Bruker AMX 400 and 500 MHz spectrophotometer using $CDCl_3$ as the solvent and TMS as an internal reference; chemical shifts (δ scale) are reported in parts per million (ppm). ^{1}H NMR spectra are reported in the order: no of hydrogens, multiplicity, and coupling constant (J value) in hertz (Hz); signals were characterized as s (singlet), d (doublet), t (triplet), m (multiplet), br s (broad singlet). ^{13}C NMR spectra were recorded at 100 and 125 MHz on a Bruker AMX 400 and 500 MHz spectrophotometer using $CDCl_3$ as the solvent. ^{1}H–^{13}C COSY spectra were was recorded on a Bruker AMX 400 NMR spectrometer using standard parameters and 0.05 M solutions of the samples prepared using $CDCl_3$ were used for recording 2D NMR spectra. The tubes used for recording NMR spectra were 5 mm in diameter. Electrospray ionization high-resolution mass spectrometry (ESI-HRMS) was carried out in a Bruker Maxis instrument at the School of Chemistry, University of Hyderabad. CHN elemental analyses were carried out on a Thermo Finnigan Flash EA 1112 analyzer at the School of Chemistry, University of Hyderabad. Routine monitoring of the reactions was performed by thin layer chromatography (TLC), using silica gel plates (Merck 60 F254), and compounds were visualized with UV light at a wavelength of 254 nm.

2.2. Synthesis of N-((1H-indol-3-yl) (phenyl) methyl) aniline derivatives

Aryl-amines (2.0 mM), aryl-aldehydes (2.0 mM) and 5-cyanoindole (2.0 mM) in the presence of glycolic acid (2.0 mM, 1.520 g) were combined and heated in 25 mL of CH_3CN at 110 °C for 5–8 h (Scheme 1). The progress of the reaction was monitored by TLC. After completion, the reaction mixture was poured onto crushed ice. The colored precipitate was filtered and washed with water. The crude product was subjected to column chromatography using hexane and ethylacetate (3:1) as the eluent.

2.2.1. 3-((4-nitrophenyl)(p-tolylamino)methyl)-1H-indole-5-carbonitrile (6)

Pink color crystals; MF: $C_{23}H_{18}N_4O_2$; mp 121–123 °C; IR (KBr) ν_{max} (cm^{-1}): 3396 (NH); ^{1}H NMR (400 MHz, $CDCl_3$): δ 2.15 (s, CH_3), 5.96 (s, methine CH), 6.56–6.58 (d, ArH), 6.85–6.87 (d, ArH), 7.07 (s, ArH), 7.34–7.36 (d, ArH), 7.48–7.51 (d, ArH), 7.73–7.75 (d, ArH), 7.99 (s, ArH), 8.15–8.17 (d, ArH), 5.87 (br s, amine-NH) 11.43 (s, indole-NH) ppm; ^{13}C NMR (100 MHz, $CDCl_3$): δ 19.96, 53.94, 101.32, 112.61, 113.11, 117.27, 120.31, 123.25, 123.87, 124.44, 125.34, 125.94,126.21, 127.21, 127.89, 129.06, 138.20, 144.80, 146.39, 150.90 ppm; HRMS (ESI-MS) Exert, M. W. 382.1430; found 383.1517 [M + H]$^+$; Elemental analysis: *Anal. Calcd:* C, 72.24; H, 4.74; N, 14.65 (%), found: C, 72.31; H, 4.67; N, 14.55 (%).

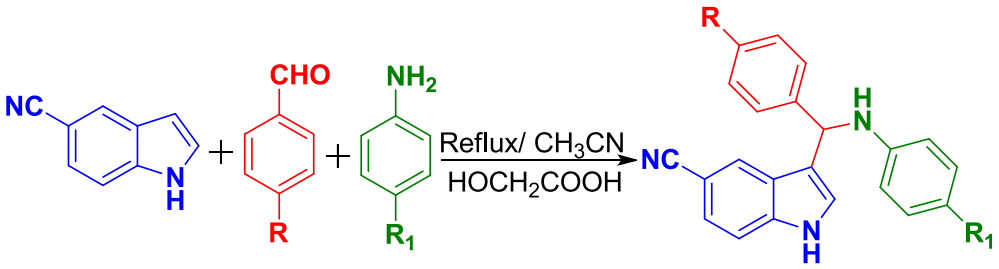

Scheme 1. Synthesis of 3-alkylindole derivatives.

2.2.2. 3-((4-methoxyphenyl)amino(4-nitrophenyl)methyl)-1H-indole-5-carbonitrile (7)

Yellow color; MF: $C_{23}H_{18}N_4O_3$; mp 169–171 °C; IR (KBr) ν_{max} (cm^{-1}): 3396 (NH); ^{1}H NMR (400 MHz, $CDCl_3$): δ 3.85 (s, 3H, OCH_3), 6.50 (s, methine CH), 6.63–6.64 (d, ArH), 6.73 (s, ArH), 6.87–6.90 (dd, ArH), 6.94–6.97 (d, ArH), 7.17–7.19 (d, ArH), 7.30–7.32 (s, ArH), 7.39–7.45 (d, ArH), 7.63–7.65 (d, ArH), 7.93–7.95 (d, ArH), 8.04–8.11 (m, ArH), 8.26–8.31 (m, ArH), 8.38–8.43 (d, ArH), 8.58–8.68 (s, ArH), 5.77 (s, amine-NH) 10.16 (s, indole-NH) ppm; ^{13}C NMR (100 MHz, $CDCl_3$): δ 43.0, 55.5, 112.3, 112.4, 114.5, 115.9, 118.4, 118.8, 120.7, 122.6, 123.7, 124.3, 125.3, 126.5, 127.6, 129.1, 130.5, 138.5, 138.9, 140.0, 141.7, 146.5, 149.0, 150.9, 154.8, 159.2 ppm; LCMS. (*m*/*z*) 398; Elemental analysis: *Anal. Calcd.* C, 69.34; H, 4.55; N, 14.06 (%), found: C, 69.34; H, 4.55; N, 14.06 (%).

2.2.3. 3-((4-methoxyphenyl)(p-tolylamino)methyl)-1H-indole-5-carbonitrile (8)

Yellow color solid; MF: $C_{24}H_{21}N_3O$; mp 97–99 °C; IR (KBr) ν_{max} (cm^{-1}): 3396 (NH); ^{1}H NMR (400 MHz, $CDCl_3$): δ 2.07 (s, 3H, CH_3), 3.89 (s, 3H, OCH_3), 5.80 (s, methine CH), 6.81–6.88 (m, ArH), 7.12–7.14 (d, ArH), 7.19–7.28 (m, ArH), 7.34–7.39 (d, ArH), 7.40 (d, ArH), 7.42–7.73 (d, ArH), 8.54 (s, indole-NH) ppm; ^{13}C NMR (100 MHz, $CDCl_3$): δ 21.0, 39.4, 55.2, 102.5, 111.4, 112.2, 113.7, 114.0, 116.5, 119.5, 120.7, 124.7, 125.5, 126.6, 128.1, 129.7, 130.1, 131.1, 134.4, 138.4, 158.4 ppm; LCMS. (*m*/*z*) 367; Elemental analysis: *Anal. Calcd.* C, 78.45; H, 5.76; N, 11.44 (%), found: C, 78.55; H, 5.70; N, 11.41 (%).

2.2.4. 3-((4-methoxyphenyl)((4-methoxyphenyl)amino)methyl)-1H-indole-5-carbonitrile (9)

Pale yellow solid; MF: $C_{24}H_{21}N_3O_2$; mp 67–69 °C; IR (KBr) ν_{max} (cm^{-1}): 3396 (NH); ^{1}H NMR (400 MHz, $CDCl_3$): δ 3.87, 3.91 (d, 6H, OCH_3), 5.93 (s, methane CH), 6.84–6.89 (m, ArH), 6.90 (s, ArH), 6.94–6.96 (t, ArH), 7.01 (s, ArH), 7.38 (s, ArH), 7.57–7.59 (d, ArH), 7.85–7.87 (s, ArH), 5.93 (s, amine-NH) 9.90 (s, indole-NH) ppm; ^{13}C NMR (100 MHz, $CDCl_3$): δ 55.3, 60.6, 113.4, 113.8, 113.9, 114.1, 114.2, 113.3, 114.4, 123.4, 126.3, 127.0, 128.5, 129.9, 130.2, 132.0, 142.8, 161.6, 164.6 ppm; LCMS. (*m*/*z*) 383; Elemental analysis: *Anal. Calcd.* C, 75.18; H, 5.52; N, 10.96 (%), found: C, 75.22; H, 5.57; N, 11.03 (%).

2.2.5. 3-((4-methoxyphenyl)((4-nitrophenyl)amino)methyl)-1H-indole-5-carbonitrile (10)

Orange colour solid; MF: $C_{23}H_{18}N_4O_3$; mp 153–155 °C; IR (KBr) ν_{max} (cm^{-1}): 3396 (NH); ^{1}H NMR (400 MHz, $CDCl_3$): δ 3.87 (s, 3H, OCH_3), 5.83 (s, methine CH), 6.61–6.63 (d, ArH), 6.80–6.82 (d, ArH), 6.84–6.86 (s, ArH), 7.34–7.36 (d, ArH), 7.48–7.51 (d, ArH), 7.73–7.75 (d, ArH), 7.99 (s, ArH), 8.15–8.17 (d, ArH), 5.87 (s, amine-NH) 9.88 (s, indole-NH) ppm; ^{13}C NMR (100 MHz, $CDCl_3$): δ 55.1, 59.4, 100.4, 112.1, 112.3, 113.1, 113.3, 113.9, 118.8, 118.9, 120.4, 123.2, 123.3, 124.2, 124.3, 124.5, 125.8, 126.0, 126.7, 128.8, 129.3, 131.4, 134.9, 136.0, 138.5, 141.9, 142.3, 144.1, 154.9, 157.5 ppm; LCMS. (*m*/*z*) 398; Elemental analysis: *Anal. Calcd.* C, 69.34; H, 4.55; N, 14.06 (%); found: C, 69.31; H, 4.47; N, 14.04 (%).

2.2.6. 3-((4-fluorophenyl)((4-methoxyphenyl)amino)methyl)-1H-indole-5-carbonitrile (11)

Pale white color; MF: $C_{23}H_{18}FN_3O$; mp 87–89 °C; IR (KBr) ν_{max} (cm^{-1}): 3387 (NH); ^{1}H NMR (400 MHz, $CDCl_3$): δ 2.22 (s, CH_3), 5.85 (s, methine CH), 6.65–6.68 (d, ArH), 7.11–7.14 (d, ArH), 7.16–7.19 (t, 1H), 7.43–7.47 (d, ArH), 7.51–7.54 (d, ArH), 5.89 (s, amine-NH) 10.43 (s, indole-NH) ppm; ^{13}C NMR (100 MHz, $CDCl_3$): δ 23.7, 53.2, 113.5, 114.5, 116.2, 121.6, 122.1, 123.5, 124.7, 125.8, 127.4, 138.7, 146.6, 163.6 ppm; LCMS. (*m*/*z*) 371; Elemental analysis: *Anal. Calcd.* C, 74.38; H, 4.88; N, 11.31 (%), found: C, 74.35; H, 5.02; N, 11.22 (%).

2.2.7. 3-((4-chlorophenyl)((4-nitrophenyl)amino)methyl)-1H-indole-5-carbonitrile (12)

Yellow color solid; MF: $C_{22}H_{15}ClN_4O_2$; mp 113–115 °C; IR (KBr) ν_{max} (cm^{-1}): 3396 (NH); ^{1}H NMR (400 MHz, $CDCl_3$): δ 2.11 (s, ArH), 5.92 (s, methine CH), 6.65 (d, ArH), 7.10–7.12 (d, ArH), 7.15–7.17 (d, 1H), 7.45–7.47 (d, ArH), 7.53 (s, ArH), 8.13–8.14 (d, ArH), 4.15 (s, amine-NH) 8.30. (s, indole-NH) ppm; ^{13}C NMR (100 MHz, $CDCl_3$): δ 21.1, 60.5, 114.3, 115.9, 117.9, 120.6, 122.9, 123.7, 124.2, 125.4, 129.4, 137.5, 146.6, 151.1 ppm; LCMS. (*m*/*z*) 402; Elemental analysis: *Anal. Calcd.* C, 65.59; H, 3.75; N, 13.91 (%), found: C, 65.61; H, 3.79; N, 13.87 (%).

2.3. Synthesis of 3,3′-(phenylmethylene)bis(1H-indole-5-carbonitrile)

A mixture of benzyamines (2.0 mM), aromatic aldehydes (2.0 mM) and 5-cyanoindole (2.0 mM) in the presence of glycolic acid (0.1410 mg) were heated in 25 mL of CH_3CN at 110 °C for 4–6 h (Scheme 2). The progress of the reaction was monitored by TLC. After completion, the reaction mixture was poured onto crushed ice. The colored precipitate was filtered and washed with water. The crude product was subjected to column chromatography using hexane and ethylacetate (3:1) as the eluent.

2.3.1. 3,3′-((4-methoxyphenyl)methylene)bis(1H-indole-5-carbonitrile) (13)

Wheat color solid; MF: $C_{26}H_{18}N_4O$; mp 147–149 °C; IR (KBr) ν_{max} (cm^{-1}): 3396 (NH); ^{1}H NMR (400 MHz, $CDCl_3$ + DMSO): δ 3.83 (s, 3H, OCH_3), 5.81 (s, methine CH), 6.78–6.83 (t, ArH), 6.98–7.00 (d, ArH), 7.17–7.19 (d, ArH), 7.26–7.28 (d, ArH), 7.44–7.48 (d, ArH), 7.59–7.62 (d, ArH), 7.77–7.79 (d, ArH), 7.95–8.00 (d, ArH), 8.57 (s, ArH) 11.27 (s, indole-NH) ppm; ^{13}C NMR (100 MHz, $CDCl_3$ + DMSO): δ 38.2, 55.1, 100.4, 104.0, 113.2, 113.4, 115.4, 118.9, 119.9, 120.4, 123.4, 124.3, 125.4, 125.9, 126.1, 126.2, 126.6, 128.9, 130.4, 132.1, 136.0, 138.3, 157.5, 161.9, 158.0 ppm; HRMS (ESI-MS) Exert, M. W.; 402.1481, found 403.1583 $[MH]^+$;

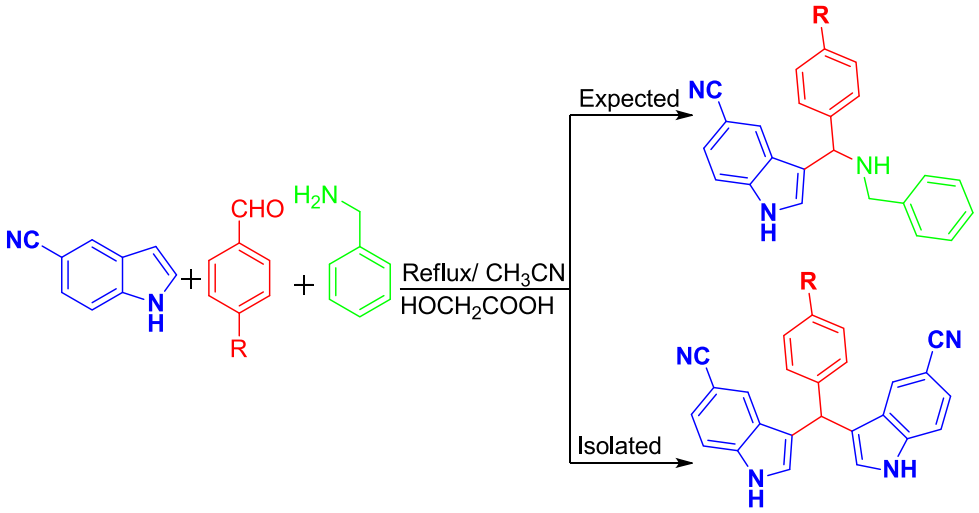

Scheme 2. Synthetic path of some 3-alkyl bis-indole compounds.

Elemental analysis: *Anal. Calcd.* C, 77.59; H, 4.51; N, 13.92 (%), found: C, 77.54; H, 4.48; N, 13.85 (%).

2.3.2. 3,3′-((4-fluorophenyl)methylene)bis(1H-indole-5-carbonitrile) (14)

White color solid; MF: $C_{25}H_{15}FN_4$; mp 153–155 °C; IR (KBr) ν_{max} (cm^{-1}): 3396 (NH); ^{1}H NMR (500 MHz, Acetone): δ, 6.14 (s, methine CH), 7.08–7.11 (d, ArH), 7.40–7.42 (d, ArH), 7.45–7.48 (t, ArH), 7.61–7.62 (d, ArH), 7.81 (s, ArH), 8.15–8.17 (m, ArH), 10.03 (s, indole-NH) ppm; ^{13}C NMR (100 MHz, Acetone): δ 38.73, 101.7, 102.4, 112.4, 112.7, 115.0, 116.0, 116.2, 119.3, 120.2, 123.9, 124.1, 124.7, 125.7, 126.7, 127.3, 130.1, 130.2, 132.1, 132.2, 138.7, 139.8, 160.5, 162.4 ppm; HRMS (ESI-MS) Exert, M. W. (390.1281); found 391.1360 $[MH]^+$. Elemental analysis: *Anal. Calcd:* C, 76.91; H, 3.87; N, 14.35 (%), found: C, 76.87; H, 3.83; N, 14.29 (%).

2.3.3. 3,3′-((4-nitrophenyl)methylene)bis(1H-indole-5-carbonitrile) (15)

Yellow color solid; MF: $C_{25}H_{15}N_5O_2$: mp 71–73 °C; IR (KBr) ν_{max} (cm^{-1}): 3373 (NH); ^{1}H NMR (500 MHz, DMSO): δ, 5.97 (s, methine CH), 7.13–7.15 (d, ArH), 7.44–7.46 (d, ArH), 7.57–7.61 (t, ArH), 7.65–7.72 (d, ArH), 7.73–7.76 (d, ArH), 8.31–8.35 (m, ArH), 11.13 (s, indole-NH) ppm; ^{13}C NMR (125 MHz, DMSO d_6): δ 38.13, 102.6, 103.7, 112.1, 112.9, 115.4, 116.7, 117.0, 119.6, 120.3, 123.8, 124.3, 124.1, 125.8, 125.9, 126.6, 130.4, 130., 132.1, 132.2, 138.7, 139.8, 147.5 ppm; LCMS. (m/z) 417; Elemental analysis: *Anal. Calcd.* C, 71.93; H, 3.62; N, 16.78 (%), found: C, 71.88; H, 3.63; N, 16.69 (%).

2.3.4. 3,3′-((4-chlorophenyl)methylene)bis(1H-indole-5-carbonitrile) (16)

Pale yellow solid; MF: $C_{25}H_{15}ClN_4$: mp 122–124 °C; IR (KBr) ν_{max} (cm^{-1}): 3369 (NH); ^{1}H NMR (400 MHz, DMSO): δ, 5.87 (s, methine CH), 6.91–6.93 (d, ArH), 7.11–7.15 (d, ArH), 7.17–7.18 (d, ArH), 7.28–7.31 (d, ArH), 7.53–7.60 (d, ArH), 7.71–7.83 (m, ArH), 5.67 (br s, amine —NH) 10.43 (s, indole-NH) ppm; ^{13}C NMR (100 MHz, DMSO): δ 38.13, 102.6, 103.7, 112.1, 112.9, 115.4, 116.7, 117.0, 119.6, 120.3, 123.8, 124.3, 124.1, 125.8, 125.9, 126.6, 130.4, 130., 132.1, 132.2, 138.7, 139.8, 147.5 ppm; LCMS. (m/z) 406; Elemental analysis: *Anal. Calcd.* C, 73.80; H, 3.72; N, 13.77 (%), found: C, 71.69; H, 3.57; N, 16.71 (%).

2.3.5. 3,3′-(p-tolylmethylene)bis(1H-indole-5-carbonitrile) (17)

Yellow color solid; MF: $C_{26}H_{18}N_4$; mp 170–172 °C; IR (KBr) ν_{max} (cm^{-1}): 3396 (NH); ^{1}H NMR (400 MHz, $CDCl_3$ + DMSO): δ 2.21 (s, CH_3), 5.79 (s, methine CH), 6.61–6.64 (t, ArH), 6.98–7.00 (d, ArH), 7.17–7.19 (d, ArH), 7.25–7.28 (d, ArH), 7.41–7.45 (d, ArH), 7.53–7.55 (d, ArH), 7.78–7.82 (d, ArH), 7.90–8.05 (d, ArH), 8.53 (s, ArH) 10.37 (s, indole-NH) ppm; ^{13}C NMR (100 MHz, $CDCl_3$ + DMSO): δ 22.7, 37.7, 101.9, 113.2, 113.4, 115.4, 118.9, 119.9, 120.4, 123.4, 124.3, 125.4, 125.9, 126.1, 126.2, 126.6, 128.9, 130.4, 132.1, 136.0, 138.3, 143.2 ppm; LCMS. (m/z) 386; Elemental analysis: *Anal. Calcd.* C, 80.81; H, 4.69; N, 14.50 (%), found: C, 80.84; H, 4.73; N, 14.55 (%).

2.3.6. 3,3′-((4-bromophenyl)methylene)bis(1H-indole-5-carbonitrile) (18)

Yellow solid; MF: $C_{25}H_{15}BrN_4$; mp 121–123 °C; IR (KBr) ν_{max} (cm^{-1}): 3401 (NH); ^{1}H NMR (400 MHz, DMSO): δ, 5.89 (s, methine CH), 6.63–6.65 (d, ArH), 7.15–7.17 (d, ArH), 7.19–7.21 (d, ArH), 7.31–7.34 (d, ArH), 7.37–7.40 (d, ArH), 7.64–7.73 (m, ArH), 5.67 (s, amine –NH) 10.33 (s, indole-NH) ppm; ^{13}C NMR (100 MHz, DMSO d_6): δ 39.01, 101.4, 113.9, 114.4, 115.9, 116.7, 118.3, 119.1, 120.6, 122.2, 125.7, 125.9, 126.7, 130.4, 131.5, 132.1, 133.6, 137.5, 139.8, 142.1 ppm; LCMS. (m/z) 450; Elemental analysis: *Anal. Calcd.* C, 66.53; H, 3.35; N, 12.41 (%), found: C, 66.53; H, 3.35; N, 12.41 (%).

2.4. Molecular docking studies

Molecular docking was performed with the *Glide* module implemented in *Maestro* version 9.3.5 of the Schrödinger software suite, 2011. The ligands were prepared with *Ligprep* in which the conformers were generated using a rapid torsion angle search approach followed by minimization of each generated structure using the OPLS-2005 (Optimized Potential for Liquid Simulations) force field. The 3D coordinates of the crystallographic structure of the 4-amino-fluro[2,3-*d*]pyrimidine PDE5A1 (PDB ID: 2H44) was downloaded from BrookhavenProtein Data Bank (www.rscb.com). The protein complex was pre-processed and prepared with *Protein Preparation Wizard* in Maestro (version 9.3.5) of the Schrödinger software suite, 2011. Minimization of the complex was continued using OPLS-2005 force field until the root mean square deviation (RMSD) reached a value of 0.3 Å. Glide provides three different levels of docking precision: high-throughput virtual screening (HTVS); standard precision (SP), and extra precision (XP).

We carried out our calculations in XP mode. The best fit molecules with the protein were ranked based on the GlideScore.

3. Results and discussion

3.1. Chemistry

After several trials, CH_3CN was found to be the most effective solvent for the reaction in terms of reaction time and yield (Table 1). In the case of aryl-aldehydes/aryl-amines with electron-withdrawing groups such as NO_2, the reaction times were reduced and the yields were increased considerably (Table 1). Due to its efficiency, simplicity and mild reaction conditions (Table 2), this procedure will be an attractive addition to the existing arsenal for the synthesis of *N*-((1H-indol-3-yl) (phenyl) methyl) aniline derivatives.

We further investigated the three-component Mannich-type reaction of 5-cyanoindole, benzylamines, and aryl-aldehyde in the presence of glycolic acid in CH_3CN as a solvent. Unfortunately, the reaction did not proceed according to our expectations, and *N*-((1H-indol-3-yl) (phenyl) methyl) aniline derivatives and bis-indole (**13**–**18**) were formed as products (Table 3). Therefore, we screened various solvents for the synthesis of 3-alkyl bis-indole (Scheme 2).

The reaction was carried out in the presence of glycolic acid under reflux for 4–8 h, and afforded compounds (**6**–**13**). All of these products were characterized by IR, ^{1}H NMR (**6**-Fig. S1, **13**-Fig. S5), ^{13}C NMR (**6**-Fig. S2, **13**-Fig. S6), HR-Mass (**6**-Fig. S4, **13**-Fig. S8) and CHN analysis. To obtain further evidence for the structure, ^{1}H–^{13}C spectra (**6**-Fig. S3, **13**-Fig. S7) of the representative compounds (**6** and **13**) were also recorded. The structures of all of the synthesized compounds (**6**–**18**) are given in Fig. 2. The structure of 3-((4-nitrophenyl) (*p*-tolylamino) methyl)-1H-indole-5-carbonitrile (Fig. 3) in the solid state was further confirmed by single-crystal X-ray diffraction analysis.

Compound **6** was obtained as pink color crystals. The ESI-HRMS analysis of the molecular ion clusters $[M + H]^+$ (*m*/*z* 383.1517) revealed the molecular formula to be $C_{23}H_{18}N_4O_2$, in conjunction with the NMR data analysis, suggesting that 13 has eleven degrees of unsaturation. Its IR spectrum revealed the strong absorption bands at 3396 cm^{-1}, corresponding to NH groups. The ^{1}H NMR spectrum of **6** (Fig. S1) showed typical proton signals for the methyl group in the toluidine moiety at 2.15 ppm. The sharp singlet at 5.96 ppm with one proton integral value should be due to the methine proton. The exchangeable amino proton appears as a broad singlet at 5.82 ppm. The *meta* and *ortho* protons of the aniline moiety appear as two separate doublets at 7.73–7.75 and 6.56–6.58 ppm, respectively. The *ortho* and *meta* protons of the aldehydic phenyl ring were observed as two doublets at 6.85–6.87 and 8.15–8.17 ppm. The indolyl protons appeared as a singlet and doublets in the region 7.07–7.99 ppm. The indolyl-NH proton appeared as a singlet in the most downfield region (11.63–8.30 ppm).

In the ^{13}C NMR spectrum of compound **6** (Fig. S2), the signal at 19.9 ppm correlated with the methyl proton singlet at 2.15 ppm, and the signal at 53.9 ppm correlated with the benzylic proton signal at 5.96 ppm. Hence, the signal at 53.9 ppm must correspond to methine (C-10) carbon. The signals at 112.6 and 124.4 ppm showed correlations with the doublets at 7.48–7.51 ppm and 7.34–7.36 ppm, respectively, due to H-6 and H-7 protons. Hence, the signals at 112.6 and 124.4 ppm were due to C-6 and C-7 carbons. Similarly, the signals at 125.9 and 126.2 ppm were correlated with the singlets at 7.99 and 7.07 ppm due to H-2 and H-4, respectively. Therefore, the signals at 125.9 and 126.2 ppm are due to C-2 and C-4 carbons of the indolyl moiety. The two signals at 113.1 and 127.8 ppm exhibited strong cross-peaks with the doublets at 6.56–6.58 and 7.73–7.75 ppm respectively due to *ortho* and *meta* protons of the aniline moiety. Hence, the signals at 113.1 and 127.8 ppm are due to the *ortho* and *meta* pair carbons of the aniline ring, respectively. The two signals at 123.2 and 129.0 ppm exhibit strong cross-peaks with the doublets pertaining to *meta* and *ortho* protons of the aldehydic phenyl ring, respectively. Therefore, the two signals at 123.2 ppm and 129.0 ppm were assigned to *meta* and *ortho* carbons of the phenyl ring of aromatic aldehyde, respectively. All of the other synthesized compounds (**7**–**12** and **14**–**18**) were characterized similarly and spectral data are presented in the experimental section.

3.2. Antimicrobial activity

All the synthesized compounds (**6**–**10**) were tested for their antibacterial activity against *Salmonella typhi*, *Staphylococcus aureus*, *Escherichia coli, Klebsiella pneumoniae and Pseudomonas aeruginosa,* as well as their antifungal activities against *Aspergillus flavus*, *Candida albicans*, *Aspergillus niger*, *and Aspergillus fumigatus*. The zones of inhibition (mm) of compounds (**6**–**10**) against all the tested microorganisms are listed in Table 4. The data indicate that compounds **6**, **7**, and **10** showed very good antibacterial activity against *S.typhi* and *S.aureus* in comparison to amikacin the standard. Fig. 4 shows the antibacterial activity graph of compounds **6**–**10** and Fig. 5 shows the antifungal activity graph of compounds **6**–**10**. However, compounds **8** and **9** showed very little activity against any of the microorganisms tested. Based on the diameter zones of inhibition shown in Table 4, it was inferred that compounds (**6**–**10**) showed very good antifungal activity against *A.niger* compared to amphotericin B as the standard, but they showed very poor activity against the other fungal strains examined. In order to support the experimentally predicted biological properties, molecular docking was carried out.

3.3. Molecular docking studies

Molecular docking is a powerful way to show how drug compounds and proteins bind to each other (Kuruvilla et al., 2019; Dhandapani et al., 2022). Docking contributes to the elucidation of the most advantageous binding posture of a ligand to its recep-

Table 1
Optimization of reaction conditions[a].

Entry	Solvent	Catalyst	R	R_1	Time (h)	Yield[b] (%)
1	DMF	$HOCH_2COOH$	NO_2	CH_3	7	53
2	Toluene	$HOCH_2COOH$	NO_2	CH_3	6	55
3	EtOH	$HOCH_2COOH$	NO_2	CH_3	7	67
4	MeOH	$HOCH_2COOH$	NO_2	CH_3	7	65
5	THF	$HOCH_2COOH$	NO_2	CH_3	8	51
6	CH_3CN	$HOCH_2COOH$	NO_2	CH_3	6	77

(2.0 mM), and *p*-methylaniline (1.2 mM) in 25 mL of solvent at reflux conditions.
[a] All the reactions were carried out using indole (2.0 mM), *p*-nitrobenzaldehyde.
[b] Isolated yield.

Table 2
The results of $HOCH_2COOH$ catalyzed synthesis of 3-alkyl indoles.

Entry	Solvent	Catalyst	R	R_1	Time (h)	Yield (%)
7	CH_3CN	$HOCH_2COOH$	NO_2	OCH_3	5	75
8	CH_3CN	$HOCH_2COOH$	OCH_3	CH_3	6	65
9	CH_3CN	$HOCH_2COOH$	OCH_3	OCH_3	6	61
10	CH_3CN	$HOCH_2COOH$	OCH_3	NO_2	5	73
11	CH_3CN	$HOCH_2COOH$	F	OCH_3	7	55
12	CH_3CN	$HOCH_2COOH$	Cl	CH_3	6	57

All the reactions were performed using 5-cyano indole (2.0 mM), aryl-aldehydes (2.0 mM) and aryl-amines (2.0 mM).

Table 3
The result of $HOCH_2COOH$ catalyzed synthesis of bis(indolyl) methane compounds.

Entry	Solvent	Catalyst	R	Time (h)	Yield (%)
13	CH_3CN	$HOCH_2COOH$	OCH_3	5	67
14	CH_3CN	$HOCH_2COOH$	F	4	81
15	CH_3CN	$HOCH_2COOH$	NO_2	6	73
16	CH_3CN	$HOCH_2COOH$	Cl	5	70
17	CH_3CN	$HOCH_2COOH$	CH_3	6	61
18	CH_3CN	$HOCH_2COOH$	Br	5	71

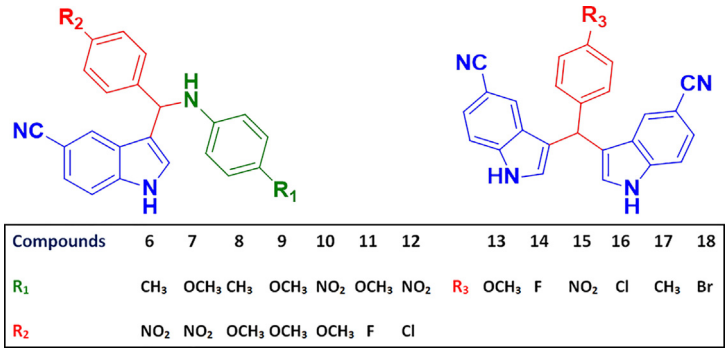

Fig. 2. Chemical structures of *N*-((1H-indol-3-yl)(phenyl)methyl)aniline derivatives.

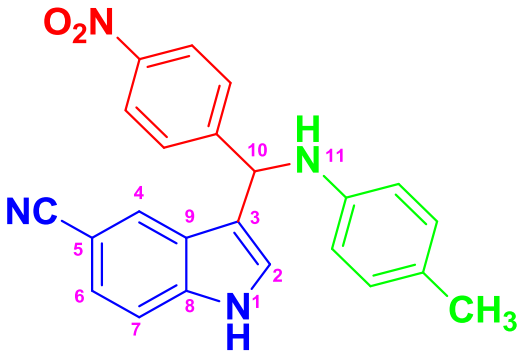

Fig. 3. Structure of compound **6**.

tor in terms of binding energy (Susan et al., 2019; Aayisha et al., 2019). The bioactivities of compounds can be determined by analysis of their interactions with a target protein (Arulraj et al., 2021). Molecular docking is an important strategy for detecting potential drug–target interactions and plays a vital role in drug discovery (Arulraj et al., 2020; Arulraj et al., 2022a; Anitha et al., 2022). Molecular docking studies were performed to find essential active site residues involved in the activity or selectivity of the newly synthesized compounds against the target fungal protein, phosphodiesterase-5 (PDE5) (PDB: 2H44) (Ahmed et al., 2012). The orientations of the inhibitors and interaction patterns were also examined, which imply the roles of various functional groups present in the lead molecule. Docking studies revealed that the inhibitors (**6–10**) interacted with active site residues of PDE5, such as MET816, PHE786, and PHE820. Histograms of compounds GlideScore values are shown in Fig. S9.

The binding mode of inhibition with 2H44–4385 is shown in Fig. 6a-e. The details of interaction and GlideScore values are presented in Table 5. Inhibitor 6 with DockScore −10.5 kcal/mole showed three kinds types of interaction: two π-π stacking interactions between the benzene ring of indole and the phenyl ring of PHE820 and PHE786, and a hydrophobic interaction with MET816. Inhibitors **8** and **9** with DockScores −10.5 and −9.7 kcal/-mol, respectively showed two π-π stacking interactions with PHE786 and PHE820.

Inhibitor **7** [dock score −10.8 kcal/mole] shows only hydrophobic interaction with MET816 but in case of ligand **10** (dock score −10.6 kcal/mole) there is only one hydrogen bond interaction between nitrogen atom of nitrile group on the indolyl moiety and hydrogen atom of water molecule. From the glide score values and binding interactions possessed by the ligands, it is very clear that all the ligand molecules are good inhibitors of the target fungal protein, phosphodiesterase-5 (PDB5) PDB: 2H44.

3.4. In silico ADMET study

ADME stands for absorption, distribution, metabolism, and excretion. The effectiveness of any given medicine in the body depends on how well it is absorbed, distributed, broken down,

Table 4
Antibacterial and antifungal activity of compounds (**6–10**) by disc diffusion method.

Compounds	*Microorganism*, Zone of inhibition (mm)								
	Antibacterial activity					Antifungal activity			
	S. typhi	*S. aureus*	*E. coli*	*K. pneumoniae*	*P. aeruginosa*	*A. flavus*	*C. albicans*	*A. fumigatus*	*A. niger*
Compound 6	1.5	2.5	1.0	1.0	2.5	2.3	2.2	2.4	2.5
Compound 7	2.2	2.4	2.5	2.1	3.1	2.4	2.8	2.4	2.9
Compound 8	3.1	2.0	2.5	2.0	1.2	2.2	2.4	2.7	2.7
Compound 9	1.0	2.0	2.0	2.0	1.2	2.4	2.7	2.3	3.1
Compound 10	2.2	2.4	2.5	2.3	3.1	3.	2.9	1.3	2.7
Amikacin	1.0	2.5	2.5	1.0	1.0	–	–	–	–
Amphotericin B	–	–	–	–	–	2.5	2.5	2.5	2.5

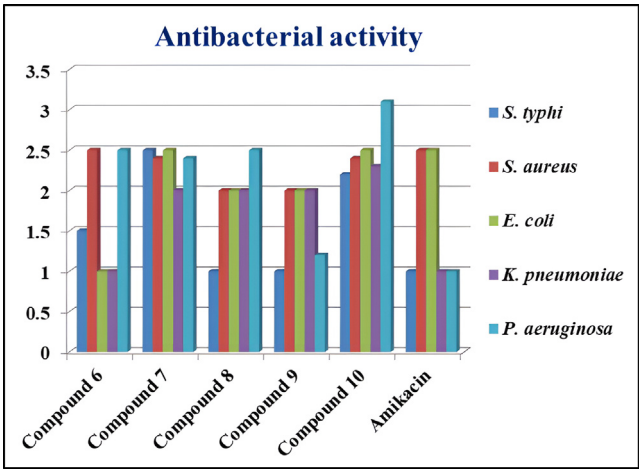

Fig. 4. Antibacterial activity graph of compounds **6–10**.

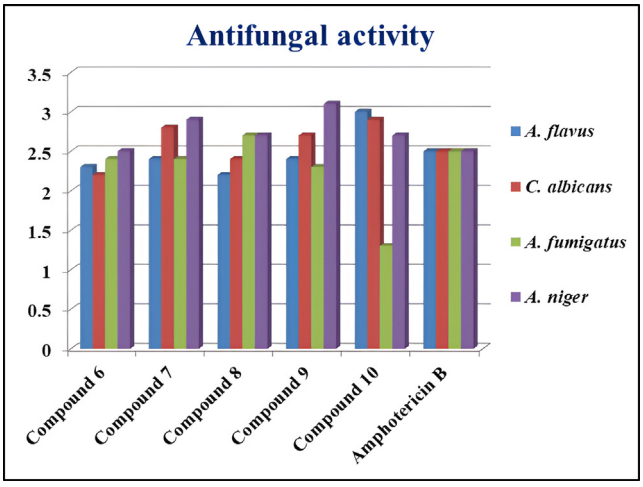

Fig. 5. Antifungal activity graph of compounds **6–10**.

and gotten rid of. SwissADME is a reliable online programme that lets you make predictions about how similar a chemical substance is to a drug and how it works in the body (Daina et al., 2017). So, the ADME properties of ligands and complexes were looked into to learn more about how a change in the structure of a complex affects its biological activity. Bioavailability radar (BR), which is often used to quickly judge how similar something is to a drug, looks at six physicochemical parameters: lipophilicity, size, polarity, solubility, flexibility, and saturation (Arulraj et al., 2022b; Arulraj et al., 2022c). The drug-likeness of a molecule is determined by its lipophilicity, the quality responsible for the passage

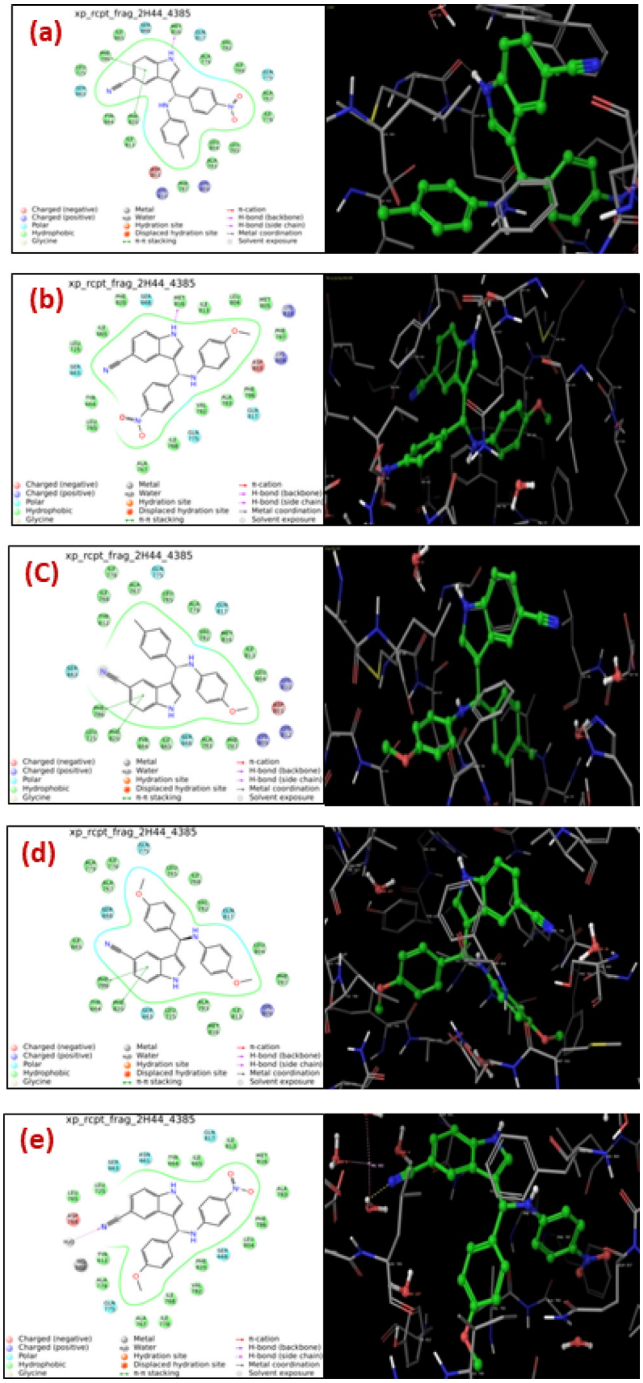

Fig. 6. (a)-(e) Molecular docking structure of 2D (left side) and 3D (right side) of compounds (**6–10**).

Table 5
Molecular docking results based on Gscore, Lipophilic EvdW, PhobEn and hydrogen bonding interactions of compounds (**6**–**10**).

Compounds	Gscore (kcal/mol)	Lipophilic EvdW	Phob En	Interacting residues of 2H44
6	−10.5	−7.7	−2.7	Phe 786, 820, Met 816
7	−10.8	−8.0	−2.7	Met 816
8	−10.5	−8.8	−2.4	Phe 786, 820
9	−9.7	−7.8	−2.0	Phe 786, 820
10	−10.6	−7.8	−2.7	H_2O

of substances over the lipid bilayer membrane of the cell to reach the site of action. Usually, the octanol–water partition coefficient is used to figure out how much a ligand moves through a membrane. This is called the permeation of the ligand (log $P_{o/w}$). The primary physicochemical properties investigated in these studies are MW (molecular weight), (2) lipophilicity, (3) HBD and HBA (number of hydrogen bond donors and acceptors), (4) number of rings, ROT (rotatable bonds), PSA (polar surface area), and (5) acid-base properties.

In this regard, we attempted to explore the chemical structural properties of compounds (**6–10**). The bioavailability radar for the ligands and complexes is shown in Fig. S10. The in silico log *P* prediction models WLOGP, XLOGP3, MLOGP, iLOGP, and Silicos-IT log P were used, and the compound (**6–10**) values are shown in Table S1. The ligand (**6**–**10**) fulfils Lipinski's rule of five. The consensus log *P* values for compounds (**6–10**) were 3.12, 2.78, 4.42, 4.06, and 2.78, respectively. All of the compounds (**6–10**) fulfil the lipophilicity requirement for becoming drugs. For compounds (**6**–**10**), the number of hydrogen bond donors (HBD) was one and the number of hydrogen bond acceptors (HBA) was 3, 3, 2, 2, and 3, while the number of bonds that may be rotated was 5, 6, 5, 6, and 6. According to the resultant data, the entire produced compounds (**6–10**) exhibit a sequence of ideal features related to high bioavailability. Compounds **6–10** that looked like drugs and were studied could be good candidates for further therapeutic development. A bioavailability score (ABS) is a measure that shows the chance that a molecule's bioavailability in rats is greater than 10 %. All ligands **6–10** demonstrated that ABS is the optimal value for a neutral molecule to behave as an effective oral medication.

3.5. Gastrointestinal absorption and Brain penetration prediction [BOILED-Egg]

Several drug development efforts failed due to insufficient pharmacology and bioavailability. Brain permeability and gastrointestinal absorption are two pharmacokinetic parameters that have been assessed at various phases of the drug development process. Brain Or IntestinaL estimated permeability approach (BOILED-Egg) was presented as an effective prediction model based on small molecule lipophilicity and polarity calculations in order to attain this objective (Daina et al., 2016). Egan et al. generated particular information based on lipophilicity and polarity to differentiate between chemicals that are well-absorbed and ones that are poorly absorbed (Egan et al., 2000). Based on a plot of two determined descriptors, PSA vs ALOGP98, the separation occurs in a region with favorable qualities for gastrointestinal absorption (Ghose et al., 1998). The BOILED-Egg model offers a rapid, simple, easily reproducible, and statistically unmatched method for predicting the excellent gastrointestinal absorption and brain permeability of tiny compounds that may be used in drug development and discovery.

Based on how it affects permeability and solubility, a drug's ability to be absorbed depends a lot on its molecular size. Here on the tPSA vs WLOGP plot (Fig. 7), the elliptical that best classifies compounds **6–10** in the HIA dataset was built to include as many well-absorbed and as few poorly absorbed compounds as practically possible. The white part of the egg (the yolk) seems to be the physicochemical zone of substances that are likely to be absorbed by the GI tract. This is called HIA permeation (human

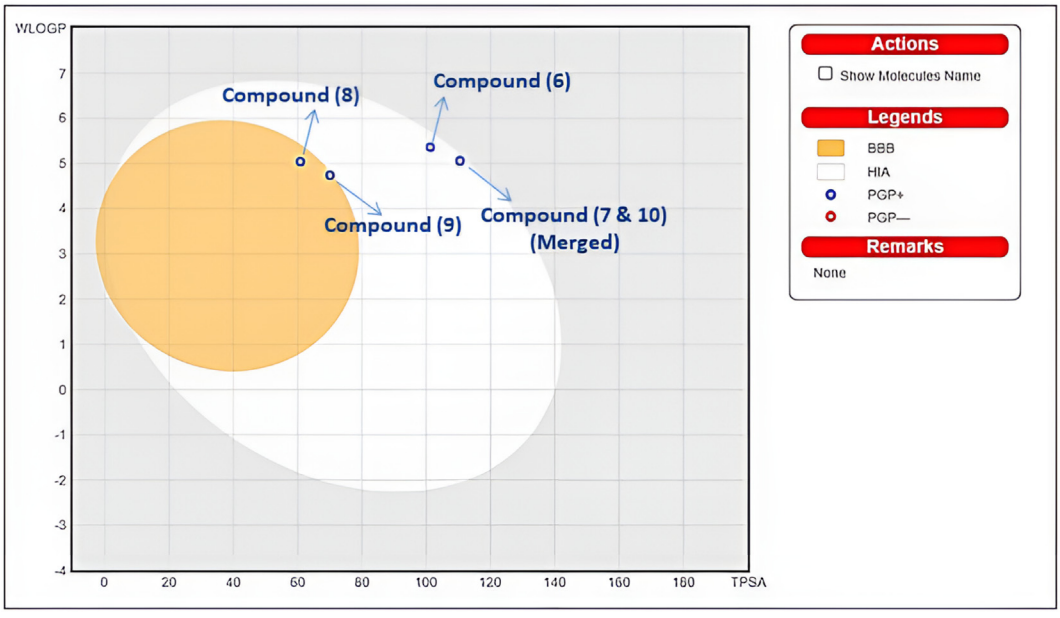

Fig. 7. BOILED-Egg predictive model for the compounds (6–10).

intestinal absorption). The Blood-Brain Barrier, shown in yellow, is a physical and chemical zone where chemicals that are likely to get into the brain (BBB permeation) are kept. As shown in Fig. 7, the compounds (**6–10**) with apparent oral bioavailability were superimposed over the BROILED-Egg. Molecules that are generally polar (PSA < 79 $Å^2$) and moderately lipophilic (log *P* between + 0.4 and + 6.0) have a high chance of getting to the CNS. The computed polarity (PSA) values for compounds **6–10** were as follows: 101.27 $Å^2$, 110.50 $Å^2$, 60.84 $Å^2$, 70.07 $Å^2$, and 110.50 $Å^2$. The calculated lipophilic values for compounds (**6**) through (**10**) are 3.12, 2.78, 4.42, 4.06, and 2.78, respectively. The estimated BOILED-Egg graphic demonstrates that our compounds (**6–10**) have improved pharmacokinetic and bioavailability properties.

4. Conclusion

We have developed a convenient and eco-friendly methodology for the synthesis of novel 3-alkylated indoles in good yields under mild reaction conditions using inexpensive, readily available, and environmentally benign glycolic acid catalyst. This new catalytic multicomponent reaction will be attractive for diversity-oriented synthesis involving C–C bond formation. This strategy has a number of advantages, including a simple work-up procedure and short reaction time. The antimicrobial experiments indicated that *para*-nitro-substituted compounds are good inhibitors of *Aspergillus niger*. The inhibitors were found to interact with active site residues, such as MET816, PHE786, and PHE820 in the target fungal protein, phosphodiesterase-5 (PDB5) (PDB: 2H44). In addition, the synthesized compounds (**6–10**) were examined for their potential as drugs using Lipinski's five rules and ADMET studies. The results indicate that the compounds (**6–10**) have remarkable pharmacological properties and therapeutic potential.

Declaration of Competing Interest

The authors declare that they have no known competing financial interests or personal relationships that could have appeared to influence the work reported in this paper.

Acknowledgements

Researchers Supporting Project number (RSP-2021/61), King Saud University, Riyadh, Saudi Arabia.

Appendix A. Supplementary material

Supplementary data to this article can be found online at https://doi.org/10.1016/j.jksus.2022.102475.

References

Aayisha, S., Renuga Devi, T.S., Janani, S., Muthu, S., Raja, M., Sevvanthi, S., 2019. DFT, molecular docking and experimental FT-IR, FT-Raman, NMR inquisitions on 4-chloro-N-(4,5-dihydro-1H-imidazol-2-yl)-6-methoxy-2-methylpyrimidin-5-amine, Alpha-2-imidazoline receptor agonist antihypertensive agent. J. Mol. Struct. 1186, 468–481. https://doi.org/10.1016/j.molstruc.2019.03.056.

Ahmed, N.S., Ali, A.H., El-Nashar, S.M., Gary, B.D., Fajardo, A.M., Tinsley, H.N., Piazza, G.A., Negri, M., Abadi, A.H., 2012. Exploring the PDE5 H-pocket by ensemble docking and structure-based design and synthesis of novel β-carboline derivatives. Eur. J. Med. Chem. 57, 329–343.

Anitha, K., Sivakumar, S., Arulraj, R., Rajkumar, K., Oluwatoba, E.O., 2022. Synthesis, molecular docking of 3-(2-chloroethyl)-2,6-diphenylpiperidin-4-one: Hirshfeld surface, spectroscopic and DFT based analyses. J. Mol. Struct. 1262,. https://doi.org/10.1016/j.molstruc.2022.132993 132993.

Arulraj, R., Sivakumar, S., Suresh, S., Anitha, K., 2020. Synthesis, Vibrational spectra, DFT calculations, Hirshfeld surface analysis and Molecular docking study of 3-chloro-3-methyl-2,6-diphenylpiperidin-4-one. Spectrochim. Acta A. 232,. https://doi.org/10.1016/j.saa.2020.118166 118166.

Arulraj, R., Sivakumar, S., Mouna, M., Omar, A.D., Noureddine, I., Marek, J.W., 2021. Study of a new piperidone as an anti-Alzheimer agent: Molecular docking, electronic and intermolecular interaction investigations by DFT method. J. King Saud Univ. – Sci. 33 (8), 101632. https://doi.org/10.1016/j.jksus.2021.101632.

Arulraj, R., Murugavel, K., Sivakumar, S., Mouna, M., Oluwatoba, E.O., Amirthaganesan, S., Noureddine, I., Nathanael, D.O., 2022a. Synthesis, spectroscopic, topological, Hirshfeld surface analysis, and anti-COVID-19 molecular docking investigation of Isopropyl 1-benzoyl-4-(benzoyloxy)-2,6-diphenyl-1,2,5,6-tetrahydropyridine-3-carboxylate. Heliyon 8 (10), e10831. https://doi.org/10.1016/j.heliyon.2022.e10831.

Arulraj, R., Nurulhuda, M., Wee Joo, C., Mouna, M., Sivakumar, S., Noureddine, I., 2022b. 3-Chloro-3-Methyl-2,6-Diarylpiperidin-4-Ones as anti-cancer agents: synthesis, biological evaluation, molecular docking, and in silico ADMET prediction. Biomolecules 12 (8), 1093. https://doi.org/10.3390/biom12081093.

Arulraj, R., Ahlam Roufieda, G., Sivakumar, S., Anitha, K., Rajkumar, K., Nourdine, B., Abdelkader, C., Manikandan, E., 2022c. Synthesis, vibrational spectra, Hirshfeld surface analysis, DFT calculations, and in silico ADMET study of 3-(2-chloroethyl)-2,6-bis(4-fluorophenyl)piperidin-4-one: a potent anti-Alzheimer agent. J. Mol. Struct. 1269,. https://doi.org/10.1016/j.molstruc.2022.133845 133845.

Babu, G., Sridhar, N., Perumal, P.T., 2000. A convenient method of synthesis of bis-indolylmethanes: indium trichloride catalyzed reactions of indole with aldehydes and Schiff's bases. Synth. Commun. 30, 1609–1614.

Campos, K.R., Woo, J.C.S., Lee, S., Tillyer, R.D., 2004. A general synthesis of substituted indoles from cyclic enol ethers and enol lactones. Org. Lett. 6, 79–82.

Daina, A., Michielin, O., Zoete, V., 2017. SwissADME: A free web tool to evaluate pharmacokinetics, drug-likeness and medicinal chemistry friendliness of small molecules. Sci. Rep. 7, 42717.

Daina, A., Zoete, V., 2016. A BOILED-Egg To Predict Gastrointestinal Absorption and Brain Penetration of Small Molecules. ChemMedChem 11 (11), 1117–1121. https://doi.org/10.1002/cmdc.201600182.

de Graaff, C., Ruijter, E., Orru, R.V.A., 2012. Recent developments in asymmetric multicomponent reactions. Chem. Soc. Rev. 41, 3969–4009.

Dhandapani, A., Veeramanikandan, S., Kumar, R.S., Almansour, A.I., Arumugam, N., Subashchandrabose, S., Suresh, J., Arulraj, R., Gajalakshmi, D., 2022. Synthesis, in vitro and in silico antitumor evaluation of 3-(2,6-dichlorophenyl)-1,5-diphenylpentane-1,5-dione: Structure, spectroscopic, RDG, Hirshfeld and DFT based analyses. J. Molecular Structure 1251,. https://doi.org/10.1016/j.molstruc.2021.132002 132002.

Dömling, A., Wang, W., Wang, K., 2012. Chemistry and biology of multicomponent reactions. Chem. Rev. 112, 3083–3135.

Egan, W.J., Merz, K.M., Baldwin, J.J., 2000. Prediction of Drug Absorption Using Multivariate Statistics. J. Med. Chem. 43, 3867–3877. https://doi.org/10.1021/jm000292e.

Garbe, T.R., Kobayashi, M., Shimizu, N., Takesue, N., Ozawa, M., Yukawa, H., 2000. Indolyl carboxylic acids by condensation of indoles with alpha-keto acids. J. Nat. Prod. 63, 596–598.

Ghose, A.K., Viswanadhan, V.N., Wendoloski, J.J., 1998. Prediction of Hydrophobic (Lipophilic) Properties of Small Organic Molecules Using Fragmental Methods: An Analysis of ALOGP and CLOGP Methods. J. Phys. Chem. A 102 (21), 3762–3772. https://doi.org/10.1021/jp980230o.

Glennon, R.A., Lee, M., Rangisetty, J.B., Dukat, M., Roth, B.L., Savage, J.E., McBride, A., Rauser, L., Hufeisen, S., Lee, D.K.H., 2000. 2-Substituted tryptamines: agents with selectivity for 5-HT(6) serotonin receptors. J. Med. Chem. 43, 1011–1018.

John Faulkner, D., 1999. Marine Natural Products. Nat. Prod. Rep. 16, 155–198.

Kuruvilla, T.K., Muthu, S., Prasana, J.C., George, J., Sevvanthi, S., 2019. Spectroscopic (FT-IR, FT-Raman), quantum mechanical and docking studies on methyl[(3S)-3-(naphthalen-1-yloxy)-3-(thiophen-2-yl)propyl]amine. J. Mol. Struct. 1175, 163–174. https://doi.org/10.1016/j.molstruc.2018.07.097.

Lézé, M.P., Le Borgne, M., Marchand, P., Loquet, D., Kogler, M., Le Baut, G., Palusczak, A., Hartmann, R.W.J., 2004. 2- and 3-[(aryl)(azolyl)methyl]indoles as potential non-steroidal aromatase inhibitors. J. Enzyme Inhib. Med. Chem. 19, 549–557.

Luk, L.Y.P., Qian, Q., Tanner, M.E., 2011. A cope rearrangement in the reaction catalyzed by dimethylallyltryptophan synthase? J. Am. Chem. Soc. 133, 12342–12345.

Nagarajan, R., Perumal, P.T., 2002. $InCl_3$ and $In(OTf)_3$ catalyzed reactions: synthesis of 3-acetyl indoles, bis-indolylmethane and indolylquinoline derivatives. Tetrahedron 58, 1229–1232.

Oh, K.B., Mar, W., Kim, S., Kim, J., Oh, M., Kim, J., Shin, D., Sim, C.J., Shinc, J., 2005. Bis (indole) alkaloids as sortase A inhibitors from the sponge Spongosorites sp. Bioorg. Med. Chem. Lett. 15, 4927–4931.

Ollevier, T., Nadeau, E., Guay-Bégin, A.A., 2006. Direct-type catalytic three-component Mannich reaction in aqueous media. Tetrahedron Lett. 47, 8351–8354.

Raston, C.L., Scott, J.L., 2000. Chemoselective, solvent-free aldol condensation reaction. Green Chem. 2, 49–52.

Reddy, A.V., Ravinder, K., Reddy, V.L.N., Goud, T.V., Ravikanth, V., Venkateswarlu, Y., 2003. Zeolite Catalyzed Synthesis of bis (Indolyl) Methanes. Synth. Commun. 33, 3687–3694.

Shaikh, R.R., Mazzanti, A., Petrini, M., Bartoli, G., Melchiorre, P., 2008. Proline-catalyzed asymmetric formal alpha-alkylation of aldehydes via vinylogous iminium ion intermediates generated from arylsulfonyl indoles. Angew. Chem. Int. Ed. 47, 8707–8710.

Sheldon, R., 2001. Catalytic reactions in ionic liquids. Chem. Commun., 2399–2407

Srivastava, N., Banik, B.K., 2003. Bismuth nitrate-catalyzed versatile Michael reactions. J. Org. Chem. 68, 2109–2114.
Sundberg, R.J., 1996. in The Chemistry of Indoles. Academic Press, New York.
Susan, A.C., Muthu, S., Prasana, J.C., Armakovic, S., Armakovic, S.J., Fathima, R.B., Geoffrey, B., David, R.H.A., 2019. Computational evaluation of the reactivity and pharmaceutical potential of an organic amine: A DFT, molecular dynamics simulations and molecular docking approach. Spectrochim. Acta A Mol. Biomol. Spectrosc. 222,. https://doi.org/10.1016/j.saa.2019.117188 117188.
Vardanyan, R.S., Hruby, V.J., 2006. Synthesis of Essential Drugs. Elsevier, Amsterdam.
Wang, Z.X., Kochanowska-Karamyan, A.J., Hamann, M.T., 2010. Marine indole alkaloids: potential new drug leads for the control of depression and anxiety. Chem. Rev. 110, 4489–4497.
Wenkert, E., Angell, E.C., Ferreira, V.F., Michelotti, E.L., Piettre, S.R., Sheu, J.H., Swindell, C.S., 1986. Synthesis of prenylated indoles. J. Org. Chem. 51, 2343–2351.
Wynne, J.H., Stalick, W.M., 2002. Synthesis of 3-[(1-Aryl)aminomethyl]indoles. J. Org. Chem. 67, 5850–5853.
Yoshiaki, N., Masato, Y., Youichi, I., Masnobu, H., Sakae, U.J., 2002. Ruthenium-catalyzed propargylation of aromatic compounds with propargylic alcohols. J. Am. Chem. Soc. 124, 11846–11847.
Zhao, J.L., Liu, L., Zhang, H.B., Wu, Y.C., Wang, D., Chen, Y.J., 2006. Three-Component friedel-crafts reaction of indoles, glyoxylate, and amine under solvent-free and catalyst-free conditions - Synthesis of (3-Indolyl)glycine derivatives. Synlett, 96–100.